

Isotropic soft-core potentials with two characteristic length scales and anomalous behaviour

Pol Vilaseca and Giancarlo Franzese

*Departament de Física Fonamental,
Facultat de Física, Universitat de Barcelona,
Diagonal 647, 08028, Barcelona, Spain.**

Abstract

Isotropic soft-core potentials with two characteristic length scales have been used since 40 years to describe systems with polymorphism. In the recent years intense research is showing that these potentials also display polyamorphism and several anomalies, including structural, diffusion and density anomaly. These anomalies occur in a hierarchy that resembles the anomalies of water. However, the absence of directional bonding in these isotropic potentials makes them different from water. Other systems, such as colloidal suspensions, protein solutions or liquid metals, can be well described by these family of potentials, opening the possibility of studying the mechanism generating the polyamorphism and anomalies in these complex liquids.

PACS numbers: 64.70.Ja, 82.70.Dd, 61.20.Ja, 64.70.qj, 65.20.De

I. INTRODUCTION

Isotropic pair interaction potentials are usually considered the prototype for simple atomic systems, such as argon. The most famous among them is the phenomenological potential proposed in 1931 by Sir John Edward Lennard-Jones (LJ)¹, commonly adopted as the textbook model for real gases. The LJ potential incorporates the short-range repulsion, due to the Pauli's quantum exclusion principle among electron orbitals, as a function $\sim 1/r^{12}$ of the distance r between the centres of mass of the atoms. It also includes the van der Waals attraction, due to instantaneous induced dipole-dipole London dispersion forces between the electron clouds, as a long-range function $\sim -1/r^6$. These two components are enough to generate a phase diagram with a gas, a liquid and a solid phase, as for neutral atoms or simple molecules. The LJ model reproduces not only the thermodynamics, but also the dynamics and the kinetics of these systems, providing for example a good starting point for studying processes such as the homogeneous nucleation of the crystal phase.

The LJ model, and similar potentials such as square wells, are useful also for more complex systems, e. g. colloidal suspensions or protein solutions. In these cases these isotropic pair interaction potentials can be used to represent the interactions between the particles of the solute when the degrees of freedom of the solvent are implicitly taken into account in the effective interaction potential. However, there are (anomalous) properties of these and other systems, e. g. liquid metals or water, that cannot be reproduced by simple potentials. It is, therefore, natural to ask if the family of isotropic potentials can be extended in such a way to describe the phase diagram of the anomalous substances.

Anomalous systems such as water and silica are network-forming liquids with strongly anisotropic interactions. However, for other systems such as liquid metals²⁻¹⁴, colloids¹⁵⁻¹⁹ or biological solutions²⁰⁻²² the use of soft-core isotropic potentials with two characteristic length scales is a particularly suitable way of constructing effective pair interactions capable of describing the anomalies of these systems. Without the pretension to complete or exhaustive coverage, here we recall some recent results about this topic. For other aspects related to soft-core potentials we remit to previous reviews²³⁻²⁵.

II. ANOMALOUS LIQUIDS

Experiments for Ga⁷, Bi²⁶, Te²⁷, S^{28,29}, Be, Mg, Ca, Sr, Ba³⁰, SiO₂, P, Se, Ce, Cs, Rb, Co, Ge¹², Ge₁₅Te₈₅³¹ and simulations for SiO₂³²⁻³⁵, S³⁶ and BeF₂³² reveal the presence of a temperature of maximum density (TMD) at constant pressure below which the density decreases when the temperature is lowered isobarically. This behavior is at variance with that of normal (or argon-like) liquids where the density monotonically increases when the temperature is decreased at constant pressure. The most famous example of liquid with this anomaly is water, whose TMD at 1 atm is at 4°C. Below the TMD the isobaric thermal expansion coefficient $\alpha_P \equiv \frac{1}{V} \frac{\partial V}{\partial T} \Big|_P$ of water assumes negative values. In normal liquids α_P is always positive because it is proportional to the (always positive) cross-fluctuation of volume and entropy. Other thermodynamic anomalies of water include the anomalous increase of isothermal volume fluctuations, proportional to the isothermal compressibility $K_T \equiv \frac{1}{V} \frac{\partial V}{\partial P} \Big|_T$, below 46°C at 1 atm and the anomalous increase of isobaric entropy fluctuations, proportional to the isobaric heat capacity $C_P \equiv T \frac{\partial S}{\partial T} \Big|_P$, below 35°C at 1 atm³⁷.

Another anomaly observed in water and other liquid is related to the diffusion coefficient D , defined as

$$D \equiv \lim_{t \rightarrow \infty} \frac{\langle \Delta r(t)^2 \rangle}{2dt} \quad (1)$$

where t is the time, $d = 3$ is the dimension of the system,

$$\langle \Delta r(t)^2 \rangle \equiv \langle [r(t_o + t) - r(t_o)]^2 \rangle \quad (2)$$

is the mean square displacement of a single particle, t_o is any time at equilibrium and the average is over the initial t_o and over the particles in the system. In a normal liquid D decreases when density ρ or pressure P are increased. Anomalous liquids, instead, are characterized by a region of the phase diagram where D increases when P is increased at constant temperature T . In the case of water, for example, experiments show that the normal behaviour of D is restored only at pressures higher than $P \approx 1.1$ kbar at 283 K³⁸.

Also the structure can be anomalous. Normal liquids tend to become more structured when compressed. This can be quantified by a translational order parameter t that measures the tendency of the molecules to adopt preferential separations, and by an orientational order parameter Q_l that measures the tendency of a molecule and its nearest neighbours to assume a specific local arrangement, as considered by Steinhardt et al.³⁹. The translational order

parameter is defined as^{34,40,41}

$$t \equiv \int_0^\infty |g(\xi) - 1| d\xi \quad (3)$$

where $\xi \equiv r\rho^{1/3}$ is a reduced distance (in units of the mean interparticle separation $\rho^{-1/3}$) and $g(\xi)$ is the radial distribution function. As the parameter t depends only on the deviations of $g(\xi)$ from unity, its value is sensible to long range periodicities. For an ideal gas $g(\xi)$ is constant and equal to 1 and there is no translational order ($t = 0$). For a crystal phase $g(\xi) \neq 1$ for long distances and t becomes large.

The orientational order parameter is by definition³⁹

$$Q_l \equiv \frac{1}{N} \sum_{i=1}^N Q_l^i \quad (4)$$

where $l = 1, 2, \dots$ is an index, $Q_l^i \equiv \left[\frac{4\pi}{2l+1} \sum_{m=-l}^{m=l} |(\bar{Y}_{lm}^i)_k|^2 \right]^{1/2}$, k is a fixed number of nearest neighbour particles and $(\bar{Y}_{lm}^i)_k \equiv \frac{1}{k} \sum_{j=1}^k Y_{lm}(r_{ij})$ is the average of the spherical harmonics Y_{lm} with indices l and m , evaluated over the vector distance r_{ij} between particles i and j . For $l = 6$ and $k = 12$, Q_6 reaches its minimum value $Q_6^{\text{ih}} = 1/\sqrt{k} = 0.287$ for an isotropic homogeneous system, while for a fully ordered f.c.c arrangement is $Q_6^{\text{fcc}} = 0.574$.

For a normal liquid t and Q_l increase with pressure. Anomalous liquids, instead, show a region where the structural order parameters decrease for increasing pressure (or density) at constant T , i.e. the system becomes more disordered. This is what has been observed, for example, in molecular dynamics simulations for water by Errington and Debendetti⁴⁰ and by Shell et al. for silica³⁴.

All the anomalies of water have a well determined sequence found in experiments³⁸ and simulations⁴⁰. In the $T - \rho$ plane the water structural anomaly region is encompassing the diffusion anomaly region which includes the density anomaly region. However in other liquids the sequence of anomalies may be different. For example, for silica the anomalous diffusion region contains the structural anomaly regions that, in turn, includes the density anomaly region³⁴.

A. Polymorphism, Polyamorphism and Liquid–liquid phase transition

Another anomaly that has received considerable attention in recent years is the possible existence of a liquid–liquid (LL) phase transition for single-component systems with a standard gas-liquid critical point. The two coexisting liquids, the high density liquid (HDL) and

the low density liquid (LDL), would differ in density and local structure, as proposed by Poole et al. in 1992⁴², based on simulations for a water model. At that time it was known that water can have more than an amorphous state⁴³, a high density amorphous (HDA) and a low density amorphous (LDA), separated by discontinuous density–change with the character of first-order phase transitions. An even higher amorphous state, the very HDA (VHDA), of water has been observed in 2001 by Loerting and coworkers⁴⁴.

This property, called polyamorphism, i.e. the occurrence of more than one amorphous state, is usually associated to the polymorphism, i.e. the occurrence of more than one crystal phase⁴⁵. Typical examples of polymorphic substances are water with at least 16 forms of ice, and carbon with diamond and graphite (made of graphene sheets, as are fullerenes and carbon nanotubes).

Direct evidences for liquid polyamorphism have been observed experimentally in phosphorous^{46–48} in 2000, triphenyl phosphite^{49–51} in 2004 and in yttrium oxide-aluminum oxide melts⁵² in 2008. Experimental data consistent with a LL phase transition have also been presented for single-component systems, besides water, such as silica^{35,53,54}, carbon⁵⁵, selenium⁵⁶, and cobalt⁵⁷, among others^{58–60}.

A LL critical point has been predicted by simulations for all the commonly used models of water, including SPC/E, ST2, TIP4P and TIP5P^{42,61}, and for specific models of phosphorous⁶², supercooled silica^{35,36,53,63}, hydrogen⁶⁴, and carbon based on molecular dynamics simulations⁶⁵. For carbon, however, subsequent *ab initio* simulations⁶⁶ and simulations for a semiempirical potential partly based on *ab initio* data⁶⁷ did not confirm this finding.

III. ISOTROPIC MODELS WITH ANOMALIES

The anomalies described in the previous section can be reproduced by using isotropic core-softened potentials. The core-softened potentials are usually characterized by a change of curvature within the repulsive range, such as a ramp or a shoulder.

- Ramp-like potentials have their softened region defined by a repulsive ramp, establishing two competing equilibrium distances, and in some cases an attractive well^{68–82}.
- Shouldered potentials are composed by a hard-core, the repulsive shoulder softening

the core, and an optional attractive well^{11,14,23,75,83–99}.

Thermodynamic anomalies have been widely reported for such potentials. Some of these anomalies depend on the details of the potentials, as we will show in the following. Among these potentials, those with an attractive part display more than one first-order phase transition.

It was after almost 40 years from the introduction of the LJ potential that Hemmer and Stell explored the idea of core-softening, often referred as core-collapse, proposing the first repulsive-ramp potential^{68,69}. They realised that by making the core more penetrable they could induce a second first-order phase transition in systems that already have one. They justified the occurrence of the second transition in a lattice gas by means of a heuristic argument based on the (particle-hole) symmetry between occupied and unoccupied cells. This argument, however, is not applicable to continuous systems where the particle-hole symmetry does not hold. Nevertheless, they showed explicitly for fluids in one dimension how a similar phenomenon could appear by softening the hard-core, finding a range of parameters for which the phase diagram displays two first order phase transitions, both ending in critical points. The kind of potentials they proposed were discontinuous. However, they argued that other analytical potentials arbitrarily close to those they considered could be constructed and the second transition would persist for such potentials. The high-density critical point was first interpreted as a solid-solid isostructural phase transition for systems such as Cs or Ce¹⁰⁰. In their original work^{68,69} Hemmer and Stell remarked that for one dimensional models with long range attraction the isobaric thermal expansion coefficient α_P can take anomalous negative values.

In 1976, Kincaid et al.^{83,84} proposed a variant of the Hemmer–Stell potential with the hard core softened by adding a finite shoulder of constant positive energy. They found at high density and pressure an isostructural phase transition. Kincaid and Stell⁴ extended this work by introducing a shouldered potential without attraction to describe solid mixtures with isostructural transitions.

After this pioneering works, several soft-core potentials have been proposed and analyzed with approximate methods or numerical simulations to study the properties of complex liquids as liquid metals, alloys, electrolytes, colloids and, to some extent, water^{2–13,15,16,101–104}.

For example, Stillinger and Weber¹⁰⁵ in 1978 used molecular dynamics simulations to study the phase behaviour of the Gaussian core model. They reported the surprising and unexpected finding that the model at equilibrium displays water-like anomalies, such as a density of maximum melting temperature, hence a region of decreasing volume upon melting, a negative thermal expansion coefficient in the fluid phase and an increase of self-diffusion upon isothermal compression.

Later, in 1991, Debenedetti et al.¹¹ showed that anomalies can occur in two-length-scales potentials also when the inner distance is attractive and the larger distance is repulsive. They showed that such a potential on a lattice can induce the formation of an open (low density) structure at low P and T . Upon heating or pressurization the open structure loses stability and collapses into a closed (denser) structure, leading to the anomaly in density and to negative α_P . A similar model on a lattice was studied by de Oliveira and Barbosa⁹⁴ finding a LL coexistence with a line of critical points. More recently Archer and Wilding¹⁰⁶ studied a different isotropic model with short range attraction and larger range repulsion, supporting the existence of a similar line of critical points.

In 1993 Head-Gordon and Stillinger^{13,101} showed that from the inversion of the radial distribution function of water is possible to deduce an effective oxygen-oxygen interaction potential that resembles a continuous version of the Stell–Hemmer shouldered potential. In 1996, Cho et al.^{107,108} extended even further the original idea of Stell and Hemmer of a potential with two length scales, by proposing a potential with an inner well and an outer well with two characteristic attractive energies separated by a local maximum. They analyzed the model in one dimension showing the presence of the density anomaly and proposed to consider it as an effective potential for the second shell of water, assuming that the first shell can be considered as part of an invariant inner core that does not play a relevant role in the anomalous density behavior of water.

In 1998, Sadr-Lahijany et al.^{86,89} considered a similar shouldered potential in two dimensions, both in the discrete and the continuous version, with a deep attractive well. The shoulder gives rise to an inner distance that is less attractive than the outer distance. They found polymorphism: a low- P triangular lattice less dense than the liquid, and a high- P square lattice denser than the liquid. Furthermore, they reported the occurrence of three anomalies: the density anomaly, the increase of isothermal compressibility upon cooling, and the diffusion anomaly. By a simplified argument in one dimension, it was shown how the in-

crease of P reduces the Gibbs free energy at the inner distance of the potential, with respect to the larger and more attractive distance, inducing the collapse to the denser structure. The interplay between the two different local structures near the freezing line was proposed as the mechanism responsible of the anomalies. This rationalization was better clarified by Wilding and Magee⁷⁵. Further studies on a continuous version of the model by Netz et al.¹⁰⁹ showed anomalous behavior in the stable region of the phase diagram if the outer minimum is deeper than the inner minimum. In the case of a deeper inner minimum, anomalous behavior occurs inside the unstable region. Nevertheless, the study of the same model in three dimensions at low T in a stable liquid state by Quigley and Probert¹¹⁰ suggests that the anomalous behavior of such model is unique to the two-dimensional case.

Also in the 1998, Jagla^{70,71} studied a version of the purely repulsive Kincaid and Stell potential by softening the core with a linear ramp, as in the original Hemmer and Stell potential. The absence of the attractive term implies the absence of the liquid-gas phase transition. Under pressurization the potential displays many crystalline polymorphs and anomaly in density. Also in this case the occurrence of these anomalies is associated to the competition between the two scales of the potential: the hard-core distance and the distance at which the interaction becomes zero. The appearance of complex ground state structures in the system is a consequence of the competition between two terms in the enthalpy H : the pressure–volume term PV leads to minimize the volume, while the soft-core repulsive term leads to maximize the interparticle distance. The different arrangements of particles in the ground state depend on the values of the pressure P and the values of the two length scales of the potential. This result was later confirmed by Kumar et al.⁷⁶ using integral-theories. Polymorphism for purely repulsive core-softened potentials was also obtained a few years later by Velasco et al. in collaboration with Hemmer and Stell^{14,111}. More recently, by using free-energy calculations, Gribova et al.⁹⁹ showed that for this potential the system exhibits the water-like density and diffusion anomaly and that the anomalies move to the region where the crystal is stable with increasing repulsive-step width.

In 1999, Jagla analyzed a slightly modified version of the Hemmer and Stell potential⁷² in three dimensions showing by simulations the appearance of water-like anomalies and predicting by theory a LL critical point. However, in the simulations the LL critical point results inaccessible due to the inevitable crystallization⁷².

In 2001, by adopting different parameters for the potential⁷³ and by analyzing a continuous version of the model⁷⁴, Jagla showed that the LL phase transition is observed in simulations in two and three dimensions, when the attraction is strong enough, while disappears if the attraction strength is approaching zero⁷⁴. In both case, however, the density displays hysteresis at low T due to mechanical metastabilities, and water-like anomalies are observed, regardless the absence of the LL critical point, showing that the presence of the anomalies is not a sufficient condition for the occurrence of the LL critical point⁷⁴. Later, Wilding and Magee observed that the locus of density maxima ends very close to the LL critical point, when this is present⁷⁵. Xu et al.^{112,113} showed that in the super-critical region of the LL critical point the dynamics changes from Arrhenius to non-Arrhenius when the line of maxima correlation length, approximated with the line of maxima of the specific heat C_P , is crossed. Caballero and Puertas¹¹⁴ studied the model by first-order perturbation theory for different choices of the attractive range, finding that the LL phase transition is attraction-driven for long ranged potentials, and is compression-driven when the interaction is shortened.

In the same year 2001, Franzese et al.⁹⁰ showed that the occurrence of the anomalies is not a necessary condition for the LL critical point. They found, by simulations and integral equation theory¹¹⁵, that a discontinuous shouldered well (DSW) potential in three dimensions, similar to that originally proposed by Kincaid et al., displays a LL coexistence, ending in a critical point, metastable with respect to the crystal. They also showed that the system does not display an anomalous behavior in density. This result suggested that the type of systems displaying the LL phase transition could be broader than what was previously hypothesized, and that experimental evidences of a LL phase transition should be sought also in systems without density anomaly. In 2004 Skybinsky et al.¹¹⁶ showed that, by changing the parameters of the DSW, the phase diagram displays a LL critical point that is stable with respect the spontaneous homogeneous crystallization. They developed a modified van der Waals equation that qualitatively reproduces the behavior of both liquid-gas and LL critical points of the model. In 2005 Malescio et al. extended the previous work to the case of large soft-core ranges, by using an integral equation approach in the hypernetted-chain approximation. They showed that only a limited range of parameters of the DSW model give rise to a phase diagram with an accessible LL critical point and that this occurs when the repulsive component of the potential equilibrates the attractive component,

in particular when the repulsive volume weighted by the repulsive energy compensates the attractive volume weighted by the attractive energy⁹¹. Lattice Monte Carlo simulations by Balladares and Barbosa⁹³ for the DSW confirmed the LL coexistence but gave a phase diagram with a line of critical points connecting the LL phase transition and the liquid-gas phase transition. This feature appears to be an artifact of the lattice, because off-lattice Monte Carlo simulations by Rzyzko et al.¹¹⁷ showed no such a line of critical points, confirming the previous results of molecular dynamics simulations and theory^{90,91,115,116} and providing an accurate estimates of the LL critical points and its exponents.

In 2003, Buldyrev and Stanley⁹² tested the idea that for any characteristic length scale in the interaction potential the system possibly displays a different liquid phase and a new LL phase transition. They added an extra discontinuous step to the soft-core of the DSW, defining a third characteristic distance. For certain values of the parameters of the potential the system presents up to three first-order phase transitions between fluids of different densities ending in critical points. The radial distribution functions $g(r)$ displays dramatic differences in structure between the low density liquid (LDL) and the high density liquid (HDL), but less pronounced differences between the HDL and the very high density liquid (VHDL). These results suggest that more critical points could be created by adding more steps to the potential and carefully selecting the parameters. However, for $k_B T$ larger than the steps of the potential, the effect of the new length scales becomes negligible and the phase diagram converges to that of a system with a continuous potential.

Nevertheless, a few years later Cervantes et al.¹¹⁸ showed, by calculating the free energy by discrete perturbation theory, that there is a range of combination of parameters of the two-scales DSW that generate a phase diagram with three critical points: between gas and liquid, between LDL and HDL, and between HDL and VHDL. The three critical points for the two-scales DSW were found also, by Artemenko et al.¹¹⁹, by analyzing the modified van der Waals equation proposed in Ref.¹¹⁶. Therefore is not necessary to add more than two length scales in the potential to reproduce phase diagrams with more than two fluid-fluid critical points. It is enough to have two characteristic length scales that compete creating a multiplicity of minima for the free energy at different P and T . These results, about the minimum conditions to reproduce polyamorphism including at least four different characteristic densities, are particularly interesting considering that experiments⁴⁴ and molecular models simulations⁶¹ show the existence of a very high density amorphous phase of water¹²⁰.

Polyamorphism and polymorphism were also studied in two dimensions in the Kincaid-Stell purely repulsive shouldered model by Malescio and Pellicane in 2003¹²¹ and in a purely repulsive potential with a shoulder and a long-range repulsive tail by Camp^{95,96}. The fluid phase at low temperature exhibits a very rich variety of structures, including chains, stripes and polygons¹²². The Camp model approximates a two-dimensional system of dipolar particles in a strong field aligned perpendicular to the plane^{123,124}.

The properties of the core-softened potentials depend on the ratio between the two characteristic scales. Yan and co-workers^{77,78} explored a range of systems going from a hard-sphere potential to a pure ramp without hard-core, finding that thermodynamic (negative α_P) and dynamic (diffusion) anomalies occur almost across the entire range, while water-like structural anomalies occur only for cases with the ratio between the two length scales comparable with that between the first two peaks of water in standard conditions. They also showed that the anomalies have the same hierarchy as in water: the density anomaly occurs within the region of diffusion anomaly, that is found within the region of structural anomaly, as observed for the SPC/E water⁴⁰. This similarity with water exists despite the lack of directionality in the isotropic potentials. The analogy with water was pushed forward by Yan et al.⁷⁹ comparing the anomalies in the super-critical region of the two scale potential with those of TIP5P water, giving new support to the initial proposal by Cho et al.¹⁰⁸ that two-scale isotropic potentials could represent an effective interaction for the second shell of water, being the first part of the core.

The water-like hierarchy was found also by de Oliveira et al.^{81,82} in three dimensions for a shouldered potential with a small attractive region, that resembles the Camp potential⁹⁵ and that has been extensively studied by Pizio et al. recently¹²⁵. These results on all these soft-core models show that orientational interactions, such as hydrogen bonding, are not a necessary condition for the presence of water-like anomalies. The anomalous features at about the temperature of the maximum density are caused by the reduction of the large empty spaces around the molecules upon compression and heating. This effect is captured by the soft-core potentials with two characteristic length scales. However, other anomalies of water at lower T , such as the liquid-liquid phase transition and the associated Widom line are not reproduced in the correct way. In particular their slope in the $P - T$ phase diagram is opposite to what is observed in molecular water models such as TIP4P. This difference implies an opposite behaviour as function of P for thermodynamic and dynamic quantities

in the supercooled regime.

All the example of potentials mentioned above have been proposed for systems going from water to colloids, to protein solutions, to liquid metals, with specific experimental cases, such as polystyrene monolayers between water and air in two dimensions¹⁷, or gallium⁷, or tellurium¹²⁶ or liquid alkaline-earth metals near the melting point³⁰ in three dimensions. The effective (pseudo)potentials representing these systems are often similar in shape, but with different details. It is therefore interesting to understand how their properties depend on the detailed features of the potential. To this goal we present in the next section a case study for a highly tunable potential that offers the opportunity to explore the properties of a large family of soft-core potentials. This potential is a continuous version of the DSW, the continuous shouldered well (CSW) potential, introduced by Franzese in 2007⁹⁷. It was shown that the CSW potential has density anomaly in three dimensions⁹⁷ and a detailed analysis by de Oliveira et al.⁹⁸ revealed also diffusion anomaly and structural anomaly with a water-like hierarchy. Recently Standaert et al.¹²⁷ have adopted this model to study the condition of anomalous (non-Gaussian) self-diffusion in a system driven out of equilibrium by intermittent length rescaling.

IV. THE CONTINUOUS SHOULDERED WELL POTENTIAL

The CSW model⁹⁷ consists of a set of identical particles interacting through the isotropic pairwise potential

$$U(r) = \frac{U_R}{1 + \exp(\Delta(r - R_R)/a)} - U_A \exp\left[-\frac{(r - R_A)^2}{2\delta_A^2}\right] + \left(\frac{a}{r}\right)^{24} \quad (5)$$

(Fig. 1) where a is the diameter of the particles, R_A and R_R are the distance of the attractive minimum and the repulsive radius, respectively, U_A and U_R are the energies of the attractive well and the repulsive shoulder, respectively, δ_A^2 is the variance of the Gaussian centered in R_A , and Δ is the parameter which controls the slope between the shoulder and the well at R_R . Varying the parameters the potential can be tuned from a repulsive shoulder to a deep double well. In particular, by increasing Δ the soft-core repulsion becomes more penetrable near the minimum of the attractive well, and the softness of the potential increases for $r > R_R$ and decreases for $r < R_R$. We fixed here the set of values $U_R/U_A = 2$, $R_R/a = 1.6$, $R_A/a = 2$, $(\delta_A/a)^2 = 0.1$, while we change Δ , considering the values $\Delta = 15, 30, 100, 300, 500$

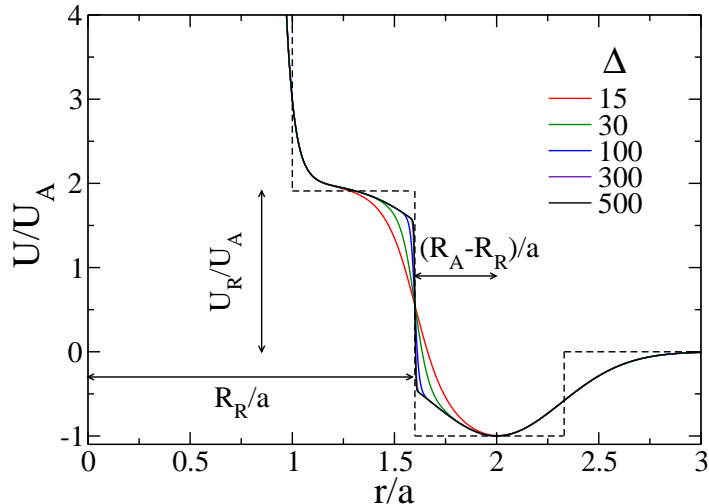


FIG. 1: The Continuous Shouldered Well (CSW) potential for $\Delta = 15, 30, 100, 300, 500$ (continuous lines) and the Discontinuous Shouldered Well (DSW) potential (dotted black line). By increasing Δ the CSW potential approximates the DSW around R_R .

(Fig. 1) going from the case $\Delta = 15$ studied in Ref.^{97,98} to slopes that approach the infinite value of DSW.

V. THE PHASE DIAGRAM

The phase diagram for all the considered values of Δ display the same qualitative behaviour in the plane $P^* - \rho^*$ (Fig. 2) where $P^* \equiv Pa^3/\epsilon$ and $\rho^* \equiv \rho a^3$ are reduced pressure and density, or $P^* - T^*$ (Fig. 3) where $T^* \equiv k_B T/\epsilon$, with k_B Boltzmann constant, is the reduced temperature. In particular, at low T^* the isotherms are non-monotonic (van der Waals loops), corresponding to the coexistence of (i) gas and liquid at low ρ^* , (ii) low density liquid (LDL) and high density liquid (HDL) at higher ρ^* . The two coexistence regions end in critical points: C_1 for gas-liquid coexistence, C_2 for LDL-HDL coexistence. For $\Delta < 100$ the HDL phase is metastable with respect to the crystal, but with a lifetime long enough to allow us to equilibrate the liquid around C_2 . For $\Delta \geq 100$ the HDL lifetime is too short to equilibrate the liquid around C_2 and we extrapolate the location of C_2 by linear fitting from higher T^* isotherms.

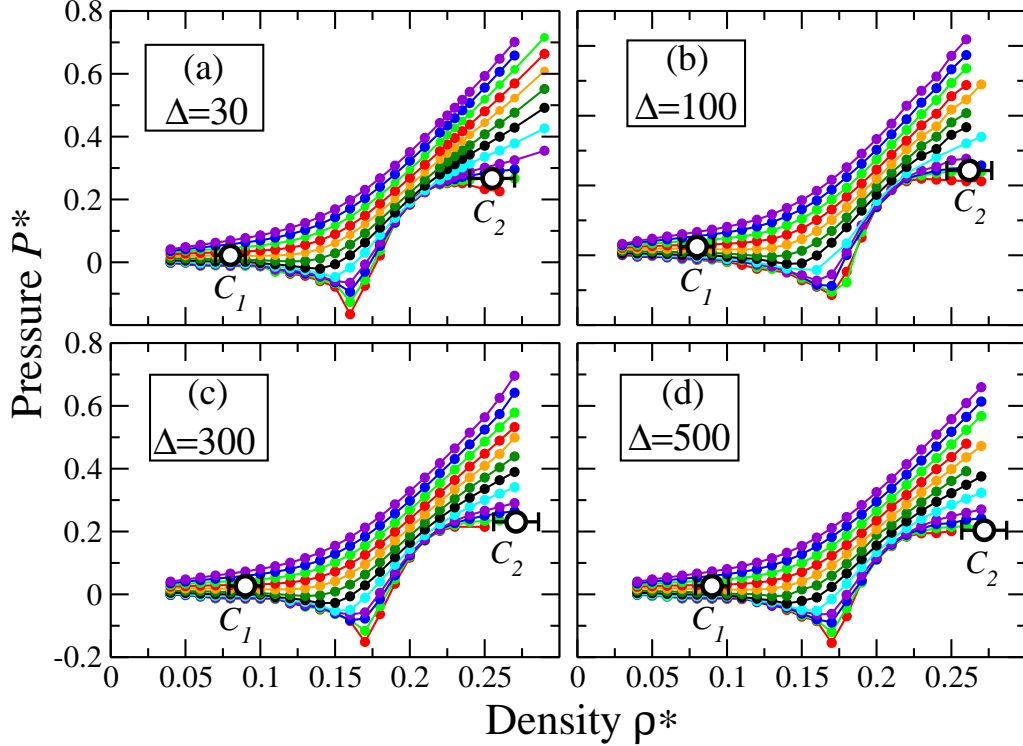


FIG. 2: Isotherms in the $P^* - \rho^*$ phase diagram from simulations for CSW potential for $\Delta = 30$ (a), $\Delta = 100$ (b), $\Delta = 300$ (c) and $\Delta = 500$ (d) (in all the panels, from top to bottom, $T^* = 1.4, 1.3, 1.2, 1.1, 1.0, 0.9, 0.8, 0.7, 0.6, 0.55, 0.5$ and 0.45).

As Δ is increased, both C_1 and C_2 tend to the corresponding values for the DSW potential. This result is consistent with the idea that the DSW can be seen as a limiting case of the family of CSW potentials presented here. However, temperature and pressure of the LDL-HDL critical point for $\Delta = 500$ ($T_{C_2}^* = 0.52 \pm 0.01$, $P_{C_2}^* = 0.204 \pm 0.007$, $\rho_{C_2}^* = 0.272 \pm 0.008$) are still far from the values for the DSW potential ($T_{C_2}^* = 0.69 \pm 0.02$, $P_{C_2}^* = 0.110 \pm 0.002$, $\rho_{C_2}^* = 0.280 \pm 0.020$).

VI. ANOMALIES

The CSW has anomalies in density, diffusion and structure. By numerical simulations, de Oliveira et al.⁹⁸ studied the case $\Delta = 15$ finding the same hierarchy of anomalies as reported for other two-scale potentials and for the SPC/E water.

In Ref.¹²⁸ we analyze in details the cases $\Delta = 30, 100, 300, 500$. In summary, for all the

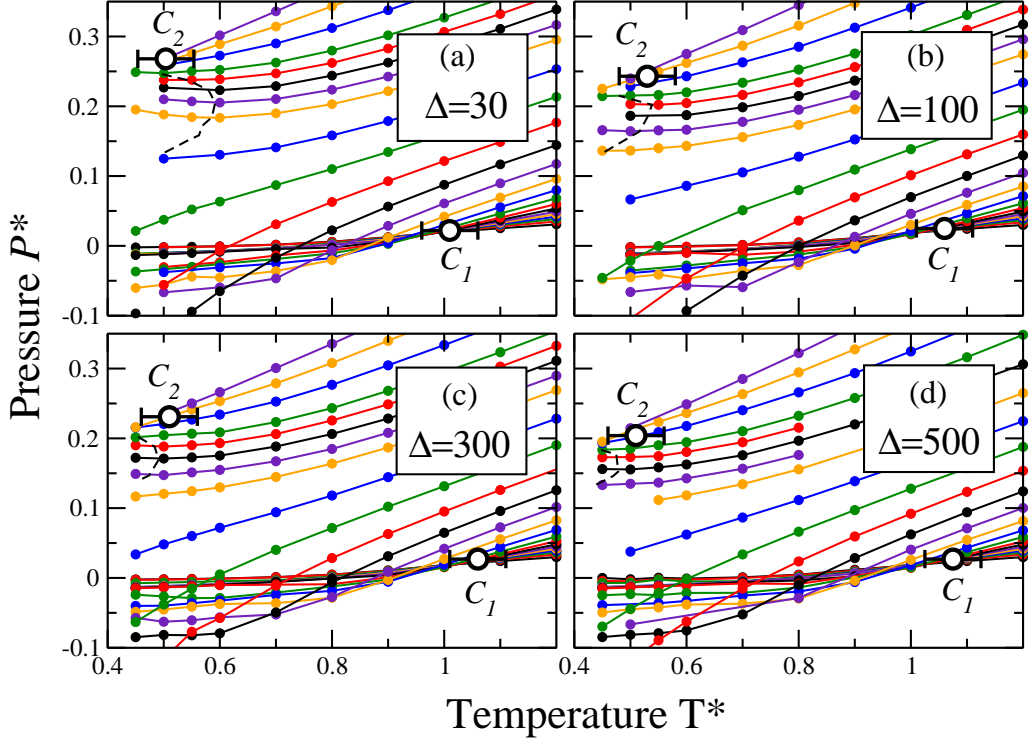


FIG. 3: The $P^* - T^*$ phase diagram for $\Delta = 30$ (a), $\Delta = 100$ (b), $\Delta = 300$ (c) and $\Delta = 500$ (d). In all the panels, we show (from bottom at $T^* = 1.2$) isochores from $\rho^* = 0.04$ to 0.20 (with constant density separation $\delta\rho^* = 0.01$), from 0.205 to 0.215 (with $\delta\rho^* = 0.005$), and from 0.22 to 0.25 (with $\delta\rho^* = 0.01$). The points where isochores cross correspond to the gas-liquid and LDL-HDL critical points (C_1 and C_2 , respectively). The black dashed line at low T is a guide for the eye estimating the TMD line, corresponding to the line of minima along the isochores.

considered values of Δ , we observe the following.

- Density anomaly.

We find a temperature of minimum pressure $(\partial P/\partial T)_\rho = 0$ along the isochores near the LDL-HDL critical point C_2 . These temperatures correspond to the TMD line at constant P , because the condition $(\partial P/\partial T)_V = 0$ implies, according to Maxwell relations, $(\partial S/\partial V)_T = 0$. Consequently, it is $(\partial S/\partial P)_T = (\partial S/\partial V)_T (\partial V/\partial P)_T = 0$ and, again using Maxwell relations, $(\partial V/\partial T)_P = (\partial \rho/\partial T)_P = 0$, which implies the presence of the temperature of maximum density (TMD) at constant P .

- Diffusion anomaly.

We find an anomalous-diffusion region, i.e. a region ($\rho_{Dmin} < \rho < \rho_{Dmax}$) where D , defined by Eq.(1), increases with increasing density at constant T .

- Structural anomaly.

We find that t , defined as in Eq.(3) increases with increasing density, for $\rho < \rho_{tmax}$, and reaches a maximum at ρ_{tmax} . Above ρ_{tmax} , for increasing ρ , t decreases until it reaches a minimum at ρ_{tmin} . For $\rho > \rho_{tmin}$, t recovers the normal behaviour.

Moreover, we observe that Q_6 , as defined in Eq.(4), has a non-monotonic behaviour along the isotherms with a maximum at ρ_{Qmax} . The density ρ_{Qmax} for each isotherm lies between ρ_{tmax} and ρ_{tmin} . In the area between ρ_{Qmax} and ρ_{tmin} both order parameters decrease for increasing ρ , hence the liquid becomes more disordered for increasing density. This behaviour defines the structural anomaly region ($\rho_{Qmax} \leq \rho \leq \rho_{tmin}$).

- Hierarchy of anomalies.

By varying the values of Δ , the regions of anomalies are affected in different ways while the hierarchy in which they occur is always preserved (Fig. 4). We find that the anomalous region where ρ decreases for decreasing T shrinks for increasing Δ and possibly tends to collapse onto one single point in the $P^* - T^*$ plane for $\Delta \rightarrow \infty$. This result would be consistent with the behaviour of the DSW potential, that does not show density anomaly^{90,91,115,116}. Also the region of the diffusion anomaly contracts as Δ increases. We find that the diffusion anomaly region always encompasses the TMD line between ρ_{Dmin} and ρ_{Dmax} (Fig. 4).

The region of structural anomaly does not contract by increasing the value of Δ but tends asymptotically to a fixed region in the $T^* - \rho^*$ plane (Fig. 4). This weak dependence on Δ suggests that the occurrence of the structural anomaly does not disappear for very steep soft-core potentials. This prediction is consistent with the excess entropy calculations that allow de Oliveira et al.⁹⁸ to argue that the structural anomaly should be observable also for the DSW potential, here considered as the limit of the CSW for $\Delta \rightarrow \infty$.

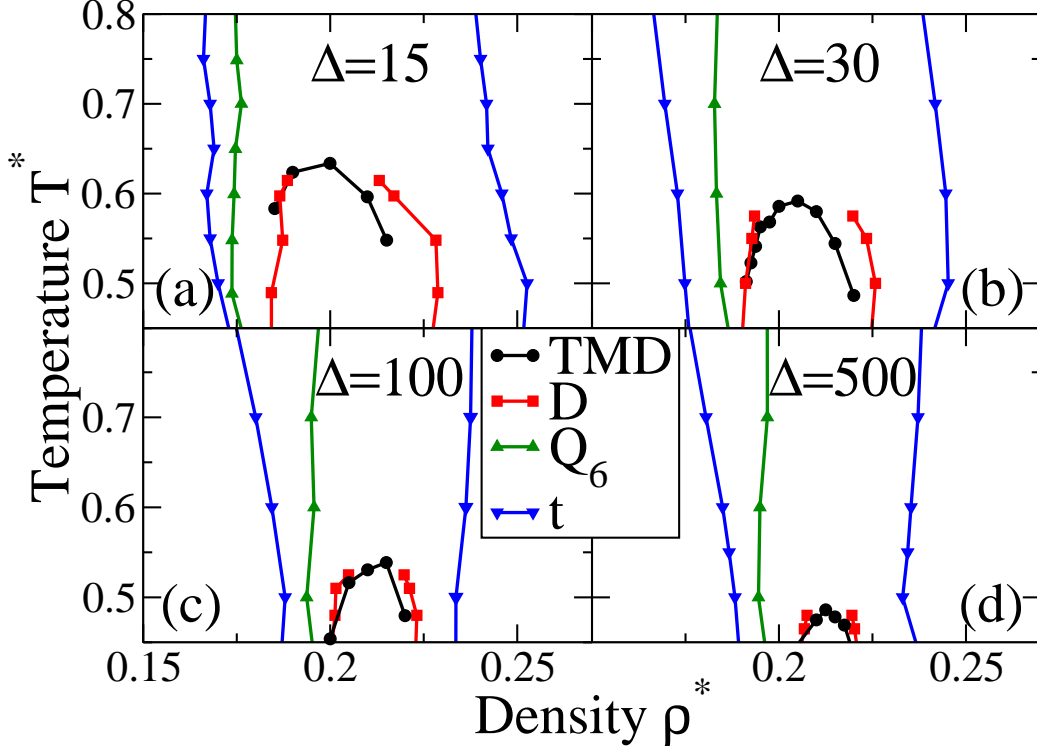


FIG. 4: Hierarchy of anomalies in the $T^* - \rho^*$ plane, plotted for (a) $\Delta = 15$, (b) $\Delta = 30$, (c) $\Delta = 100$ and (d) $\Delta = 500$. As the value of Δ increases, both the regions of density anomaly and diffusion anomaly contract, with the diffusion anomaly region always encompasses the TMD line. The region of structural anomaly is only weakly affected.

VII. OUTLOOK

Isotropic soft-core potentials with two characteristic distances are able to display the complex behaviour of anomalous liquids. They can describe the effective interactions of systems such as colloids, protein solutions or liquid metals. Due to the lack of directional interactions, these potentials provide a mechanism for the anomalies that is alternative to the bonding of network-forming liquid, e. g. water. As a consequence, their use as coarse-grained models of water is seriously disputed. In particular, they have a P -dependence of the structural fluctuations and a supercooled phase diagram that are different from those found in simulations of molecular models of water, such as SPC/E, ST2, TIP4P, TIP5P (see for example⁶¹) or of other coarse-grained water models with explicit hydrogen bond interactions^{129–132}. This wrong P -dependence affects, not only the supercooled state, but

also properties at ambient T , such as the velocity of sound. Water sound propagation shows a discontinuity in P that has a negative slope in the P - T phase diagram at 293 K and 0.29 GPa¹³³, consistent with the slope of the maxima of structural fluctuations found at the same T and P in numerical simulations of TIP4P-water by Saitta and Datchi¹³⁴. Nevertheless, the isotropic soft-core potentials with two characteristic distances display a sequence of anomalies that is water-like.

To elucidate their properties we have presented here the case of the CSW potential whose anomalous behaviour is affected by the parameter Δ associated to the steepness of the repulsive shoulder. For all the considered values of Δ , the phase diagram displays two first-order phase transitions, corresponding to a liquid-gas phase transition at low densities and a liquid-liquid phase transition at higher densities, both ending in critical points. For $15 \leq \Delta \leq 500$ we verify that the anomalies in density, diffusion and structure are in the same hierarchy as in water. We show that, as the value of Δ increases, the regions of density and diffusion anomaly contract in the $T - \rho$ plane, while the region of structural anomaly is weakly affected.

Since by increasing Δ the CSW potential approaches the discontinuous shouldered well potential (DSW), the contraction of the density anomaly and diffusion anomaly for $\Delta \rightarrow \infty$ is consistent with the fact that for the DSW potential no TMD is observed. Our results suggest that the structural anomalies, instead, should be present also in the DSW potential. Therefore, the isotropic soft-core potential with two characteristic distances can be considered as the prototype for anomalous liquids with no directional bonding. The fact that its properties depend in a dramatic way on the details of the potential calls for further investigations to understand better the mechanisms that regulates the appearance of the anomalies.

Acknowledgments

We thank MICINN-FEDER (Spain) grant FIS2009-10210 for support.

* Electronic address: pvilaseca@correu.ffn.ub.es, gfranzese@ub.edu

¹ J. E. Lennard-Jones, Proc. Camb. Phil. Soc. **27**, 469 (1931).

- ² M. Silbert and W. H. Young, Phys. Lett. A **58**, 469 (1976).
- ³ D. A. Young and B. J. Alder, Phys. Rev. Lett. **38**, 1213 (1977).
- ⁴ J. M. Kincaid and G. Stell, J. Chem. Phys. **67**, 420 (1977).
- ⁵ D. Levesque and J. J. Weis, Phys. Lett. A **60**, 473 (1977).
- ⁶ J. M. Kincaid and G. Stell, Phys. Lett. A **65**, 131 (1978).
- ⁷ K. K. Mon, N. W. Ashcroft, and G. V. Chester, Phys. Rev. B **19**, 5103 (1979).
- ⁸ P. T. Cummings and G. Stell, Mol. Phys. **43**, 1267 (1981).
- ⁹ A. Voronel, I. Paperno, S. Rabinovich, and E. Lapina, Phys. Rev. Lett. **50**, 247 (1983).
- ¹⁰ G. Kahl and J. Hafner, Solid State Comm. **49**, 1125 (1984).
- ¹¹ P. G. Debenedetti, V. S. Raghavan, and S. Borick, J. Phys. Chem. **95**, 4540 (1991).
- ¹² P. G. Debenedetti, *Metastable liquids: concepts and principles*, Princeton University Press, 7th edition ed., 1998.
- ¹³ F. H. Stillinger and T. Head-Gordon, Phys. Rev. E **47**, 2484 (1993).
- ¹⁴ E. Velasco, L. Medeiros, G. Navascués, P. C. Hemmer, and G. Stell, Phys. Rev. Lett. **85**, 122 (2000).
- ¹⁵ S. H. Behrens, D. I. Christl, R. Emmerzael, P. Schurtenberger, and M. Borkovec, Langmuir **16**, 2566 (2000).
- ¹⁶ C. N. Likos, Physics Reports **348**, 267 (2001).
- ¹⁷ M. Quesada-Perez, A. Moncho-Jorda, F. Martinez-Lopez, and R. Hidalgo-Alvarez, J. Chem. Phys. **115**, 10897 (2001).
- ¹⁸ A. Yethiraj and A. van Blaaderen, Nature (London) **421**, 513 (2003).
- ¹⁹ M. M. Baksh, M. Jaros, and J. T. Groves, Nature (London) **427**, 139 (2004).
- ²⁰ S. Brandon, P. Katsonis, and P. G. Vekilov, Phys. Rev. E **73**, 061917 (2006).
- ²¹ P. G. Vekilov, W. Pan, O. Gliko, P. Katsonis, and O. Galkin, *Aspects of Physical Biology*, volume 752 of *Lecture Notes in Physics*, chapter Metastable Mesoscopic Phases in Concentrated Protein Solutions, pages 65–95, Springer Berlin / Heidelberg, 2008.
- ²² S. Buldyrev, *Aspects of Physical Biology*, volume 752 of *Lecture Notes in Physics*, chapter Application of Discrete Molecular Dynamics to Protein Folding and Aggregation, pages 97–131, Springer Berlin / Heidelberg, 2008.
- ²³ S. V. Buldyrev, G. Franzese, N. Giovambattista, G. Malescio, M. R. Sadr-Lahijany, A. Scala, A. Skibinsky, and H. E. Stanley, Physica A **304**, 23 (2002).

- ²⁴ G. Malescio, *J. Phys.: Condens. Matter* **19** (2007).
- ²⁵ P. Kumar, G. Franzese, S. V. Buldyrev, and H. E. Stanley, *Aspects of Physical Biology*, volume 752 of *Lecture Notes in Physics*, chapter Dynamics of Water at Low Temperatures and Implications for Biomolecules, pages 3–22, Springer Berlin / Heidelberg, 2008.
- ²⁶ P. Lamparter, S. Stieb, and W. Knoll, *Z. Naturforsch A* **31**, 90 (1976).
- ²⁷ H. Thurn and J. Ruska, *J. Non-Cryst. Solids* **22**, 331 (1976).
- ²⁸ G. E. Sauer and L. B. Borst, *Science* **158**, 1567 (1967).
- ²⁹ S. J. Kennedy and J. C. Wheeler, *J. Chem. Phys.* **78**, 1523 (1983).
- ³⁰ J. F. Wax, R. Albaki, and J. L. Bretonnet, *Phys. Rev. B* **62**, 14818 (2000).
- ³¹ T. Tsuchiya, *J. Phys. Soc. Jpn.* **60**, 227 (1991).
- ³² C. A. Angell, R. D. Bressel, M. Hemmatti, E. J. Sare, and J. C. Tucker, *Phys. Chem. Chem. Phys.* **2**, 1559 (2000).
- ³³ R. Sharma, S. N. Chakraborty, and C. Chakravarty, *J. Chem. Phys.* **125**, 204501 (2006).
- ³⁴ M. S. Shell, P. G. Debenedetti, and A. Z. Panagiotopoulos, *Phys. Rev. E* **66**, 011202 (2002).
- ³⁵ P. H. Poole, M. Hemmati, and C. A. Angell, *Phys. Rev. Lett.* **79**, 2281 (1997).
- ³⁶ S. Sastry and C. A. Angell, *Nature Mater.* **2**, 739 (2003).
- ³⁷ G. Franzese and H. E. Stanley, *J. Phys.: Condens. Matter* **19**, 205126 (2007).
- ³⁸ C. A. Angell, E. D. Finch, and P. Bach, *J. Chem. Phys.* **65**, 3065 (1976).
- ³⁹ P. J. Steinhardt, D. R. Nelson, and M. Ronchetti, *Phys. Rev. B* **28**, 784 (1983).
- ⁴⁰ J. R. Errington and P. D. Debenedetti, *Nature (London)* **409**, 318 (2001).
- ⁴¹ J. E. Errington, P. G. Debenedetti, and S. Torquato, *J. Chem. Phys.* **118**, 2256 (2003).
- ⁴² P. H. Poole, F. Sciortino, U. Essmann, and H. E. Stanley, *Nature (London)* **360**, 324 (1992).
- ⁴³ O. Mishima, L. Calvert, and E. Whalley, *Nature (London)* **314**, 76 (1985).
- ⁴⁴ T. Loerting, C. Salzmann, I. Kohl, E. Mayer, and A. Hallbrucker, *Phys. Chem. Chem. Phys.* **3**, 5355 (2001).
- ⁴⁵ M. C. Wilding, M. Wilson, and P. F. McMillan, *Chem. Soc. Rev.* **35**, 964 (2006).
- ⁴⁶ Y. Katayama, T. Mizutani, W. Utsumi, O. Shimomura, M. Yamakata, and K. Funakoshi, *Nature (London)* **403**, 170 (2000).
- ⁴⁷ Y. Katayama, Y. Inamura, T. Mizutani, W. Yamakata, M. Utsumi, and S. O., *Science* **306**, 848 (2004).
- ⁴⁸ G. Monaco, F. S., W. A. Crichton, and M. Mezouar, *Phys. Rev. Lett.* **90**, 255701 (2003).

- 49 R. Kurita and H. Tanaka, *Science* **306**, 845 (2004).
- 50 H. Tanaka, R. Kurita, and H. Mataka, *Phys. Rev. Lett.* **92**, 025701 (2004).
- 51 R. Kurita and H. Tanaka, *J. Phys.: Condens. Matter* **17**, L293 (2005).
- 52 G. N. Greaves, M. C. Wilding, S. Fearn, D. Langstaff, F. Kargl, S. Cox, Q. V. Van, O. Majerus, C. J. Benmore, R. Weber, C. M. Martin, and L. Hennes, *Science* **322**, 566 (2008).
- 53 C. A. Angell, S. Borick, and M. Grabow, *J. Non-Cryst. Solids* **207**, 463 (1996).
- 54 D. J. Lacks, *Phys. Rev. Lett.* **84**, 4629 (2000).
- 55 M. van Thiel and F. H. Ree, *Phys. Rev. B* **48**, 3591 (1993).
- 56 V. V. Brazhkin, E. L. Gromnitskaya, O. V. Stalgorova, and A. G. Lyapun, *Rev. High Pressure Sci. Technol.* **7**, 1129 (1998).
- 57 M. G. Vasin and V. I. Ladýanov, *Phys. Rev. E* **68**, 051202 (2003).
- 58 S. Aasland and P. F. McMillan, *Nature (London)* **369**, 633 (1994).
- 59 M. C. Wilding and P. F. McMillan, *J. Non-Cryst. Solids* **293**, 357 (2001).
- 60 M. C. Wilding, C. J. Benmore, and P. F. McMillan, *J. Non-Cryst. Solids* **297**, 143 (2002).
- 61 I. Brovchenko, A. Geiger, and A. Oleinikova, *J. Chem. Phys.* **123**, 044515 (2005).
- 62 T. Morishita, *Phys. Rev. Lett.* **87**, 4659 (2001).
- 63 F. Saika-Voivod, F. Sciortino, and P. H. Poole, *Phys. Rev. E* **63**, 011202 (2001).
- 64 S. Scandolo, *Proc. Natl. Acad. Sci. U.S.A.* **100**, 3051 (2003).
- 65 J. N. Glosli and F. H. Ree, *Phys. Rev. Lett.* **82**, 4659 (1999).
- 66 C. J. Wu, J. N. Glosli, G. Galli, and F. H. Ree, *Phys. Rev. Lett.* **89**, 135701 (2002).
- 67 L. M. Ghiringhelli, J. H. Los, E. J. Meijer, A. Fasolino, and D. Frenkel, *Phys. Rev. Lett.* **94**, 145701 (2005).
- 68 P. C. Hemmer and G. Stell, *Phys. Rev. Lett.* **24**, 1284 (1970).
- 69 G. Stell and P. C. Hemmer, *J. Chem. Phys.* **56**, 4274 (1972).
- 70 E. A. Jagla, *Phys. Rev. E* **58**, 1478 (1998).
- 71 E. A. Jagla, *J. Chem. Phys.* **110**, 451 (1999).
- 72 E. A. Jagla, *J. Chem. Phys.* **111**, 8980 (1999).
- 73 E. A. Jagla, *Phys. Rev. E* **63**, 061501 (2001).
- 74 E. A. Jagla, *Phys. Rev. E* **63**, 061509 (2001).
- 75 N. B. Wilding and J. E. Magee, *Phys. Rev. E* **66**, 031509 (2002).
- 76 P. Kumar, S. V. Buldyrev, F. Sciortino, E. Zaccarelli, and H. E. Stanley, *Phys. Rev. E* **72**,

- 021501 (2005).
- ⁷⁷ Z. Yan, S. V. Buldyrev, N. Giovambattista, and H. E. Stanley, *Phys. Rev. Lett.* **95**, 130604 (2005).
- ⁷⁸ Z. Yan, S. V. Buldyrev, N. Giovambattista, P. G. Debenedetti, and H. E. Stanley, *Phys. Rev. E* **73**, 051204 (2006).
- ⁷⁹ Z. Yan, S. V. Buldyrev, P. Kumar, N. Giovambattista, and H. E. Stanley, *Phys. Rev. E* **77**, 042201 (2008).
- ⁸⁰ H. M. Gibson and N. B. Wilding, *Phys. Rev. E* **73**, 061507 (2006).
- ⁸¹ A. B. de Oliveira, P. A. Netz, T. Colla, and M. C. Barbosa, *J. Chem. Phys.* **124**, 084505 (2006).
- ⁸² A. B. de Oliveira, P. A. Netz, T. Colla, and M. C. Barbosa, *J. Chem. Phys.* **125**, 124503 (2006).
- ⁸³ J. M. Kincaid, G. Stell, and C. K. Hall, *J. Chem. Phys.* **65**, 2161 (1976).
- ⁸⁴ J. M. Kincaid, G. Stell, and E. Goldmark, *J. Chem. Phys.* **65**, 2172 (1976).
- ⁸⁵ C. K. Hall and G. Stell, *Phys. Rev. A* **7**, 1679 (1973).
- ⁸⁶ M. R. Sadr-Lahijany, A. Scala, S. V. Buldyrev, and H. E. Stanley, *Phys. Rev. Lett.* **81**, 4895 (1998).
- ⁸⁷ M. R. Sadr-Lahijany, A. Scala, S. V. Buldyrev, and H. E. Stanley, *Phys. Rev. E* **60**, 6714 (1999).
- ⁸⁸ A. Scala, M. R. Sadr-Lahijany, N. Giovambattista, S. V. Buldyrev, and H. E. Stanley, *J. Stat. Phys.* **100**, 97 (2000).
- ⁸⁹ A. Scala, M. R. Sadr-Lahijany, N. Giovambattista, S. V. Buldyrev, and H. E. Stanley, *Phys. Rev. E* **63**, 041202 (2001).
- ⁹⁰ G. Franzese, G. Malescio, A. Skibinsky, S. V. Buldyrev, and H. E. Stanley, *Nature (London)* **409**, 692 (2001).
- ⁹¹ G. Malescio, G. Franzese, A. Skibinsky, S. V. Buldyrev, and H. E. Stanley, *Phys. Rev. E* **71**, 061504 (2005).
- ⁹² S. V. Buldyrev and H. E. Stanley, *Physica A* **330**, 124 (2003).
- ⁹³ A. L. Balladares and M. C. Barbosa, *Journal of Physics: Condensed Matter* **16**, 8811 (2004).
- ⁹⁴ A. B. de Oliveira and M. C. Barbosa, *J. Phys.: Condens. Matter* **17**, 399 (2005).
- ⁹⁵ P. J. Camp, *Phys. Rev. E* **68**, 061506 (2003).

- ⁹⁶ P. J. Camp, Phys. Rev. E **71**, 031507 (2005).
- ⁹⁷ G. Franzese, J. Mol. Liq. **136**, 267 (2007).
- ⁹⁸ A. B. de Oliveira, G. Franzese, P. A. Netz, and M. C. Barbosa, J. Chem. Phys. **128**, 064901 (2008).
- ⁹⁹ N. V. Gribova, Y. D. Fomin, D. Frenkel, and V. N. Ryzhov, Phys. Rev. E **79**, 051202 (2009).
- ¹⁰⁰ R. I. Beecroft and C. A. Swenson, J. Phys. Chem. Solids **15**, 234 (1960).
- ¹⁰¹ T. Head-Gordon and F. H. Stillinger, J. Chem. Phys. **98**, 3313 (1993).
- ¹⁰² F. H. Stillinger and D. K. Stillinger, Physica A **244**, 385 (1997).
- ¹⁰³ M. C. Bellissent-Funel, editor, *Hydration Processes in Biology. Theoretical and Experimental Approaches*, volume 305 of *NATO Advanced Studies Institute, Series A: Life Sciences*, IOS Press, 1998.
- ¹⁰⁴ G. W. Robinson, S. Singh, S.-B. Zhu, and M. W. Evans, *Water in Biology, Chemistry and Physics*, World Scientific, 1996.
- ¹⁰⁵ F. H. Stillinger and T. A. Weber, J. Chem. Phys. **68**, 3837 (1978).
- ¹⁰⁶ A. J. Archer and N. B. Wilding, Phys. Rev. E **76**, 031501 (2007).
- ¹⁰⁷ C. H. Cho, S. Singh, and G. W. Robinson, Faraday Discuss. **103**, 19 (1996).
- ¹⁰⁸ C. H. Cho, S. Singh, and G. W. Robinson, Phys. Rev. Lett. **76**, 1651 (1996).
- ¹⁰⁹ P. A. Netz, J. F. Raymundi, A. S. Camera, and M. C. Barbosa, Physica A **342**, 48 (2004).
- ¹¹⁰ D. Quigley and M. I. J. Probert, Phys. Rev. E **71**, 065701 (2005).
- ¹¹¹ P. C. Hemmer, E. Velasco, L. Medeiros, G. Navascués, and G. Stell, J. Chem. Phys. **114**, 2268 (2001).
- ¹¹² L. Xu, P. Kumar, S. V. Buldyrev, S.-H. Chen, P. Poole, F. Sciortino, and H. E. Stanley, Proc. Natl. Acad. Sci. U.S.A. **102**, 16558 (2005).
- ¹¹³ L. Xu, S. Buldyrev, C. A. Angell, and H. E. Stanley, Phys. Rev. E **74**, 031108 (2006).
- ¹¹⁴ J. B. Caballero and A. M. Puertas, Phys. Rev. E **74**, 051506 (2006).
- ¹¹⁵ G. Franzese, G. Malescio, A. Skibinsky, S. V. Buldyrev, and H. E. Stanley, Phys. Rev. E **66**, 051206 (2002).
- ¹¹⁶ A. Skibinsky, S. V. Buldyrev, G. Franzese, G. Malescio, and H. E. Stanley, Phys. Rev. E **69**, 061206 (2004).
- ¹¹⁷ W. Rzyško, O. Pizio, A. Patrykiewicz, and S. Sokolowski, J. Chem. Phys. **129**, 124502 (2008).
- ¹¹⁸ L. A. Cervantes, A. L. Benavides, and F. del Río, J. Chem. Phys. **126**, 084507 (2007).

- ¹¹⁹ S. Artemenko, T. Lozovsky, and V. Mazur, *J. Phys.: Condens. Matter* **20**, 44119 (2008).
- ¹²⁰ T. Loerting and N. Giovambattista, *J. Phys: Cond. Mat.* **18**, R919 (2006).
- ¹²¹ G. Malescio and G. Pellicane, *Nature Mater.* **2**, 97 (2003).
- ¹²² P. D. Duncan and P. J. Camp, *J. Chem. Phys.* **121**, 11322 (2004).
- ¹²³ N. Osterman, D. Babič, I. Poberaj, J. Dobnikar, and P. Zihlerl, *Phys. Rev. Lett.* **99**, 248301 (2007).
- ¹²⁴ J. Dobnikar, J. Fornleitner, and G. Kahl, *J. Phys.: Condens. Matte* **20**, 494220 (2008).
- ¹²⁵ O. Pizio, H. Dominguez, Y. Duda, and S. Sokółowski, *J. Chem. Phys.* **130**, 174504 (2009).
- ¹²⁶ J. Hafner, *J. Phys.: Condens. Matter* **2**, 1271 (1990).
- ¹²⁷ S. Standaert, J. Ryckebusch, and L. De Cruz, Creating conditions of anomalous self-diffusion in a liquid with molecular dynamics (preprint arxiv:0907.1856v2), 2009.
- ¹²⁸ P. Vilaseca and G. Franzese, Softness dependence of the anomalies for the continuous shouldered well potential (preprint arxiv:1004.3186v1), 2010.
- ¹²⁹ P. Kumar, G. Franzese, and H. E. Stanley, *Phys. Rev. Lett.* **100**, 105701 (2008).
- ¹³⁰ M. G. Mazza, K. Stokely, E. G. Strelakova, H. E. Stanley, and G. Franzese, *Comp. Phys. Comm.* **180**, 497 (2009).
- ¹³¹ F. d. l. Santos and G. Franzese, Influence of intramolecular couplings in a model for hydrogen-bonded liquids, volume 1091, pages 185–197, Granada (Spain), 2009, AIP.
- ¹³² K. Stokely, M. G. Mazza, H. E. Stanley, and G. Franzese, *Proc. Natl. Acad. Sci. U.S.A.* **107**, 1301 (2010).
- ¹³³ F. Li, Q. Cui, Z. He, T. Cui, J. Zhang, Q. Zhou, G. Zou, and S. Sasaki, *J. Chem. Phys.* **123**, 174511 (2005).
- ¹³⁴ A. M. Saitta and F. Datchi, *Phys. Rev. E* **67**, 020201 (2003).